

Application of pulsed and high-frequency electron paramagnetic resonance techniques to study petroleum disperse systems

M.R. Gafurov^{1*}, A.A. Ponomarev², G.V. Mamin¹, A.A. Rodionov¹, F.F. Murzakhanov¹,
T. Arash¹, S.B. Orlinskii¹

¹Kazan Federal University, Kazan, Russian Federation

²Tyumen Industrial University, Tyumen, Russian Federation

Abstract. The spectral and relaxation characteristics of “free” organic radicals (FR) and vanadyl-porphyrin (VP) complexes in various petroleum disperse systems (PDS) like bitumen, petroleum, their high-molecular components and solutions were studied using stationary (conventional) and pulsed electron paramagnetic resonance (EPR) techniques in two frequency ranges (X- and W-bands, with the microwave radiation frequencies of about 9 GHz and 95 GHz, respectively). The features of the pulsed approaches (electron spin echo, modulation of the electron spin echo signal decay, electronic relaxation times) and high-frequency EPR for PDS investigations were examined. W-band EPR allows to resolve spectrally the lines from the different paramagnetic centers and more accurately determine their spectral characteristics. It is shown that the electron spin echo can be observed at room temperatures even at high magnetic fields of 3.4 T demonstrating the potential of application of pulsed EPR techniques for the low-cost oilfield measurements. Analysis of the VP transverse magnetization decay curve permits to identify electron-nuclear interactions with the ¹⁴N and ¹H nuclei *in situ* while in the EPR spectra these hyperfine interactions usually cannot be detected. It is found from the W-band EPR measurements that FR lineshape cannot be fitted with isotropic parameters in contrast to the established X-band results. The observed effect of increasing the rates of electronic transverse relaxation in asphaltenes is described in the framework of a model of spectral diffusion between the fast- and slow-relaxing paramagnetic centers in supramolecular complexes of asphaltenes.

Keywords: electron paramagnetic resonance, petroleum disperse systems, asphaltenes

Recommended citation: Gafurov M.R., Ponomarev A.A., Mamin G.V., Rodionov A.A., Murzakhanov F.F., Arash T., Orlinskii S.B. (2020). Application of pulsed and high-frequency electron paramagnetic resonance techniques to study petroleum disperse systems. *Georesursy = Georesources*, 22(4), pp. 2–14. DOI: <https://doi.org/10.18599/grs.2020.4.2-14>

1. Introduction

From the standpoint of colloid chemistry, petroleum can be considered as a complex multicomponent mixture that, depending on external conditions, exhibits the properties of a molecular solution or a disperse system (Syunyaev, 1980; Syunyaev et al., 1990; Safieva, 2004). Petroleum disperse systems (PDS) contain resins, asphaltenes that are prone to self-association and other solid particles. The study of properties and complex behavior of such a complexly organized multicomponent system is still a priority for fundamental science and oil technologies (Syunyaev, 1980; Syunyaev et al., 1990; Safieva, 2004).

PDS can contain up to 10²⁰ paramagnetic centers (PCs) per 1 gram of substance (Yen, Chilingarian, 1994, 2000). Most PCs are concentrated in high-molecular components of PDS, such as asphaltenes, resins, and polycyclic aromatic hydrocarbons. The mass content of such high-molecular components can reach 45% for petroleum and 75% for bitumen (Yen, Chilingarian, 1994, 2000). This means that in asphalt/tar materials (ATM) with an average molecular weight of 1000 Da one can find of up to one unpaired electron per molecule (Yen, Chilingarian, 1994). Obviously, such a high concentration of PCs can affect both the magnetic and electrophysical properties of PDS (Dolomatov et al., 2018). The study of both hydrocarbon and other types of PCs can provide additional information about the presence and concentration of hydrocarbons in petroleum-containing rocks, the structure and properties of PDS, which is due to the practical need for effective exploration, production, transportation and deeper

*Corresponding author: Marat R. Gafurov
E-mail: marat.gafurov@kpfu.ru

© 2020 The Authors. Published by Georesursy LLC

This is an open access article under the Creative Commons Attribution 4.0 License (<https://creativecommons.org/licenses/by/4.0/>)

processing of hard-to-recover hydrocarbon reservoirs, heavy (high-viscous) oil, bitumen, etc. (Martyanov et al., 2017).

The existence of PCs in PDS is caused by the presence of d-metals (mainly V, Ni, Fe, Mn) and stable organic “free” radicals (FR). As a rule, PCs are concentrated in asphaltenes, due to the presence of delocalized π -electrons of aromatic rings and carbon radicals of side alkane chains. The exact position and structure of the FR in PDS is still the subject of scientific discussion. The presence of heteroatoms (S, N, O) significantly expands the nomenclature of PCs, complicating their unambiguous identification. In this question, researchers traditionally refer to the work on the study of PC in anthracite (Yen, Chilingarian, 2000).

Often, especially in heavy (high-viscous) oil and bitumen, the presence of vanadium is detected (up to tenths of a percent). It is considered established (Piccinato et al., 2012) that vanadium is present in the PDS mainly in the form of vanadyl porphyrin (VP) complexes and is concentrated mostly in the ATM with predominance in asphaltenes (Figure 1).

Aggregation of asphaltenes and formation of asphaltene deposits cause serious problem for the extraction, transportation and processing of PDS attracting interest to the study of their structure and properties. Information about the participation of VP complexes in the processes of asphaltene aggregation is quite controversial (Zhao et al., 2016). There are “free” VP complexes (having a small size and simple structure), which are easily removed from asphaltenes, and “tightly bound” vanadyl porphyrins, which are bound to asphaltene molecules either covalently or through multiple intermolecular interactions (Zhao et al., 2016; Abyzgildin, 1977). Vanadium, in turn, is considered to be the main element that poisons catalysts, a metal that interferes with petroleum cracking and causes equipment wear (during the combustion of vanadium-containing fuels, adhesion- and corrosion-active inorganic vanadium compounds are one of the main causes of intensive ash drift and corrosion of high-temperature surfaces). Additional interest in studying of the structural and dynamic characteristics of petroporphyrins and other PCs has recently been associated with the possibility of using native and

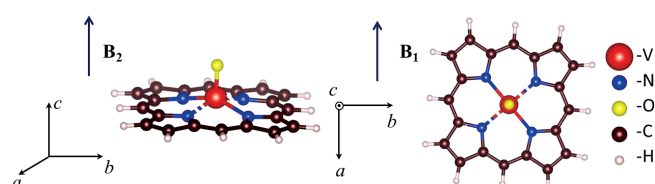


Fig. 1. Schematic representation of a single vanadyl porphyrin molecule. The values of the external magnetic fields corresponding to the orientations “in-plane” (B_1) and “out-of-plane” (B_2) are shown

impurity PCs as polarizing agents for amplifying the signal of nuclear magnetic resonance (NMR) and NMR logging from the protons of PDS using various mechanisms of dynamic nuclear polarization (DNP) for geological exploration and fundamental study of the structure of asphaltenes (Gizatullin et al., 2018, 2019; Alexandrov et al., 2019; Sapunov et al., 2016, 2019; Davydov et al., 2018; Zhang et al., 2020).

Electron Paramagnetic Resonance (EPR) has long been known as one of the most informative methods for detecting and identifying PCs in PDS, measuring their concentration, and establishing the structure of paramagnetic complexes (Khasanova et al., 2017). The method does not require additional sample preparation (for example, by dilution, as for the optical measurements), is non-destructive (unlike, for example, chromatographic/mass spectrometric methods), and allows one to study solid (bitumen) and liquid (oil) samples. EPR investigations can be performed both on PDS components and their solutions including *in situ* conditions.

Nowadays the main tools for EPR research are the X-band spectrometers operating at the microwave (MW) frequency of $\nu_{MW} = 9-10$ GHz in continuous wave (CW) mode (low-power microwave radiation is constantly applied to the sample) (Qin, Warncke, 2015a, b). Surprisingly, the technical capabilities of modern, commercially available EPR techniques (by exploiting other MW frequency ranges and pulsed approaches) are still not widely used for PDS investigations being actively utilized for decoding the structures of complex biomolecules (Qin, Warncke, 2015a, b). Until now, the vast majority of EPR experiments on PDS were limited to the methods first presented in 1950–1970s (Yen, Chilingarian, 1994; Zhang et al., 2020; Trukhan et al., 2014; Wang et al., 2016; Dolomatov et al., 2016; Garif’yanov, Kozyrev 1956; Gutowsky et al., 1958; O’Reilly, 1958; Il’yasov et al., 1961; Il’yasov 1962; Yen et al., 1962; Murav’ev et al., 2006; Yakubov et al., 2017). Only since recently an increased interest to the PDS investigation by high-frequency and pulsed EPR techniques has arisen (Ramachandran et al., 2015; Tayeb Ben et al., 2015; Mamin et al., 2016; Gracheva et al., 2016).

The purpose of this work was to study the capabilities of pulse (X- and W-bands, where for the W-band $\nu_{MW} = 94-96$ GHz) and high-frequency (W-band) EPR for PDS research. Investigations have been conducted on equipment of the Institute of Physics of Kazan Federal University (Kazan, Russia).

2. Materials and methods

2.1. Materials

From the set of the various studied PDS, several samples were selected for this work, which differ greatly in viscosity and content of high-molecular components.

| | Density at $t = 20^{\circ}\text{C}$, kg/m^3 | Viscosity at 20°C , $\text{Pa}\cdot\text{s}$ | Asphaltenes, % | Resins, % | Saturated and aromatic hydrocarbons, % |
|---------------|--|---|----------------|-----------|---|
| Ashalchinskoe | 968 | 2.48 | 3.9 | 31.0 | 65.1 |
| Salym | 827 | 0.005 | 0.1 | 3.3 | 96.4 |
| Cuban | 1029 | 270 | 17.3 | 42.8 | 39.9 |
| | ($t = 36^{\circ}\text{C}$) | | | | |
| Chinese | 920 | 1.18 | 0.6 | 10.4 | 89 |

Table 1. Rheological parameters and component composition of the samples Ashalchinskoe, Salym, Cuban and Chinese petroleum investigated in this work.

Table 1 shows the rheological parameters and component composition of petroleum from the Ashalchinskoe oilfield (Republic of Tatarstan, Russia), the Salym oilfield (Bazhenov horizon, Khanty-Mansi Autonomous Okrug-Yugra, Russia), Boca de Jaruco (Republic of Cuba) and petroleum from the Chinese oilfield. Details of group (SARA) and rheological measurements, as well as results obtained by other analytical tools for these samples can be found in (Gizatullin et al., 2018, 2019; Vakhin et al., 2020; Nesterov et al., 2019; Ponomarev, 2019).

We have also investigated 12 different asphaltene powders extracted from the technical bitumen from two petroleum refineries (samples N1 and N2). and heavy oils (samples N3 and N4) from the Akanskoe oilfield (Khanty-Mansi Autonomous Okrug-Yugra, Russia). The initial fraction of asphaltenes (designated as A_{init}) was obtained from the oils and bitumen by extraction in a Soxhlet apparatus using petroleum ether (boiling point $40\text{--}70^{\circ}\text{C}$). Further, according to the scheme of fractional precipitation of asphaltenes from solutions in toluene, the initial asphaltenes A_{init} were divided into two fractions: $A1$ – falling out of the toluene solution with adding of 65% of petroleum ether as a precipitator; and $A2$ – falling out with a maximum (90%) addition of petroleum ether (Table 2). It is assumed that the $A1$ fraction consists mainly of asphaltene molecules of the “continental” type, and $A2$ – of the “archipelago” type (Acevedo et al., 2010).

2.2. Methods

All measurements presented in this paper were performed using the capabilities of the ESP 300 and Eleksys 680 (Bruker, Germany) X- and W-bands EPR spectrometers available at the KFU Institute of Physics (Kazan, Russia). For temperature measurements,

nitrogen and helium flow cryostat were used to change the temperature of the sample in the ranges from 77 to 800 K and from 6 to 300 K, respectively.

The main design elements of CW EPR spectrometers have remained unchanged since the installation of Evgeny K. Zavoisky (Zavoisky, 1945). Typically, PDS samples are placed in a quartz or glass tube, which is then inserted into an EPR resonator located in an external magnetic field B_0 . The simplest microwave resonator can be a rectangular or cylindrical metal waveguide closed on both sides, whose geometric dimensions correspond to the microwave wavelengths. In fact, the resonator is an analog of LC circuit used in NMR. Its purpose is to accumulate energy and separate the electric and magnetic components of the microwave field, since the EPR effect is caused by interaction with the magnetic component of the electromagnetic wave, while the electric part can cause undesirable heating of the sample (Eaton et al., 2010). The standard size of the PDS sample in the X-band is 3–4 mm in diameter and 4–30 mm in height. Measurements in the W-band require a much smaller volume of the substance (tubes with a diameter of 0.1–0.8 mm, sample length 3–10 mm), which can be considered as an additional advantage of measuring specimens of limited size, studying inhomogeneous samples, series of PDS samples after thermal and catalytic treatments, etc. (Al-Muntaser et al., 2020; Mehrabi-Kalajahi et al., 2018; Galukhin et al., 2018; Mukhamatdinov et al., 2020).

To increase the sensitivity of EPR spectrometers, B_0 is modulated by a sinusoidal signal with a frequency of 10–100 kHz and a small amplitude (0.01–1 mT). In this case, the signal measured by the detector is amplitude-modulated at the modulation frequency, and the amplitude of its main harmonic is usually proportional to the first derivative of the absorption line. Thus, the PC

| Sample | Content of asphaltenes, mass. % | Number of fractions of extracted asphaltenes, mass. % | |
|--------|------------------------------------|---|------|
| | | $A1$ | $A2$ |
| N1 | 34 | 83 | 15 |
| N2 | 30 | 66 | 6.5 |
| N3 | 9.2 | 60 | 7 |
| N4 | 11.0 | 60 | 10 |

Table 2. The content of asphaltene fractions in samples N1–N4.

concentration can be determined by double integration of the recorded spectrum.

EPR spectra in both CW and pulsed modes are affected by several types of interactions of the unpaired electron with its environment:

- (1) Zeeman interaction between an unpaired electron and the external magnetic field,
- (2) the spin-orbital interaction,
- (3) electron-nuclear hyperfine interaction, or HFI,
- (4) interaction with other unpaired electrons (spin-spin interaction).

In the X-band, and especially in the W-band, the most significant contribution is the Zeeman interaction, which determines the position of the resonance lines (Yen, Chilingarian, 1994):

$$h\nu_{\text{MW}} = g\beta B_0, \quad (1)$$

where h is the Planck constant, g is the spectroscopic splitting factor, and β is the Bohr magneton.

The spin-orbital and spin-spin interactions lead to a deviation of the spectroscopic g -factor from the known value for the free electron ($g_e = 2.0023$). The typical range of g -factors in PDS varies from 1.96 (for VO^{2+}) to 2.008 for oxygen- and sulfur-containing FR (Yen, Chilingarian, 1994, 2000; Khasanova et al., 2017). To meet the resonance condition (1), a B_0 of about 0.35 T for the X-band and 3.5 T for the W-band must be applied. Thus, high-frequency PDS studies require the use of superconducting magnets, which increases the cost of measurements. A number of oil-bearing rocks contain complexes of iron group Fe^{3+} ions with a characteristic signal in the region of “half” magnetic fields ($g \approx 4.3$), as well as signals from stable sulfur- and oxygen-containing radicals (Khasanova et al., 2017).

The interaction of an unpaired electron with the nuclear magnetic moment of the nucleus (nuclei) leads to the splitting of electronic energy levels, forming the so-called hyperfine structure (HFS) of the EPR spectrum. Each m_s electron level is split into a group of $(2I+1)$ closely spaced levels, where I is a nuclear spin. Allowed transitions that contribute to the HFS of the EPR spectrum are only those transitions for which the conditions $\Delta m_s = \pm 1$ and $\Delta m_l = 0$ are met. The distance between the adjacent lines of the HFS spectrum is called the HFI constant, denoted as A .

It was shown in (Dickson et al., 1972) that the values of the parameters g and A can be used to clarify the nature of paramagnetic centers in the PDS and determine the origin of the VP complex. So, for the ligand environment of vanadium VOS_4 , the g -factor values are higher, and the A value is lower compared to VON_4 , VON_2O_2 or VOO_4 . This fact continues to be used in a number of studies to control the processes of PDS desulfurization (Cui et al., 2017, 2018), for example, although the changes in the parameters of EPR spectra observed in the X-band experiments are very small.

The use of pulse techniques significantly expands the capabilities of the EPR method and, to a large extent, complements the information extracted from CW EPR spectra. In contrast to CW EPR, in which continuous exposure of microwave radiation reveals a picture of splitting the energy levels of a paramagnetic system, pulsed EPR techniques can shed light on the dynamic behavior of the system, measure relaxation times, decipher complex spectra of interacting to each other PCs, etc. By using pulse techniques, it is often possible to identify the nature and determine the values of electron-nuclear interactions, which due to their small values compared to the width of the EPR lines cannot be resolved in the CW EPR spectra.

The pulse mode allows one to register the spectra obtained either by the free induction decay signal (FID) or by the electron spin echo (ESE) method. The FID signal in most PDS, as in most solids, quickly damps due to the spin dephasing under conditions of inhomogeneous line broadening caused by natural causes, or it is not observed at all due to the “resonator ringing” (the so-called “dead time” of the device). Therefore, pulse experiments are performed at the low Q -factor mode of the resonator, which reduces the sensitivity of EPR measurements in comparison with the CW regime.

The shape of the spectra recorded in this way (the amplitude or integral values of FID or ESE signals) usually coincides with the absorption spectra. In some cases, for example, when studying light petroleum, it may be necessary to slow down the electron relaxation processes by lowering the sample temperature in order to detect ESE spectra with an acceptable signal-to-noise ratio.

The EPR pulse spectrometer includes an additional block – a pulse driver connected to a microwave generator. Similar to NMR applications, microwave pulses can be combined into special sequences where the delay time and pulse duration are configurable parameters. However, the values of these times for electrons are 3-6 orders of magnitude shorter than in NMR, which is due to the corresponding difference in the relaxation times of electrons and nuclei. Below some used pulse sequences (with rectangular pulses) and the values of their parameters for experiments in the X-band on PDS are given.

1) A two-pulse sequence $\pi/2-\tau-\pi$ with a $\pi/2$ -pulse duration of 16 ns and a delay time $\tau = 200$ ns was used for detecting of ESE.

2) The signal of the primary ESE amplitude decay and the transverse relaxation time T_{2c} were measured using a two-pulse scheme presented above with an increase in the interval τ between pulses with a step $\Delta\tau$ of 4 ns and fixed pulse durations. A three-pulse sequence was also used to register the modulation of the Electron Spin

Echo Envelope Modulation (ESEEM) $\pi/2-(\tau_1+\Delta\tau)-\pi/2-(\tau_2+\Delta\tau)-\pi/2$ (Dikanov, Tsvetkov, 1992; Dzyuba, 2013), where $\tau_2 = 5300$ ns.

3) The recovery curve of the longitudinal magnetization and the longitudinal relaxation time T_{1e} were measured by the inversion-recovery pulse sequence of $\pi-T_{Delay}-\pi/2-\tau-\pi$ -ESE for a fixed pulse duration and time τ , but varying the T_{Delay} time.

3. Result and discussions

3.1.EPR of oil samples

Figure 2 shows the CW EPR spectra of Cuban oil at room temperature in the X-and W-band. The obtained spectra are due to the following signals: (1) single line due to signal from a FR ($g = 2.003$, peak-to-peak line width $\Delta B_{pp} \approx 6.4$ G); (2) HFS of the VO^{2+} complex with g-factor of axial symmetry ($I = 7/2$ for ^{51}V nuclei, $g_{||} = 1.963$, $g_{\perp} = 1.985$, $A_{||} = 468$ MHz, $A_{\perp} = 150$ MHz, section 3.2.); (3) HFS of Mn^{2+} ions in a carbonate rock with an isotropic g-factor ($I = 5/2$ for ^{55}Mn nuclei, $g = 2.001$, $A_{iso} = 260$ MHz; splitting is observed on the central transition of the fine structure $c \Delta m_s = (-1/2)-(+1/2)$). Due to a small difference in the values of the g-factors for the presented spin systems, the signals from

these PCs are partially spectrally resolved in the W-band. For the samples from the Salym oilfield and Chinese oil only FR signals were registered. Below we will discuss in detail the signals from the VP complexes and FR, which are typical for most of the PDS studied. Table 3 shows data on the concentration of the above-mentioned PCs extracted from the X-band CW EPR.

3.2. Study of spectral and relaxation characteristics of signals from the VP complexes

The spectral characteristics of the VP complexes of axial symmetry in the studied samples are given above (section 3.1) and are almost identical for all the specimens studied. It is possible to achieve an isotropic EPR spectrum for VP complexes in PDS by dissolving samples in organic solvents or increasing the temperature/pressure (Trukhan et al., 2014). Figure 3 shows the temperature dependence of CW EPR spectrum of the VP complex of the Ashalchinskoe oil sample in the X-band. At $T_{start} < 480$ K, a powder spectrum (16 lines) is observed, which can be described in the framework of a rotational model with a rotational correlation time $\tau_{corr} > 5 \times 10^{-7}$ s. At $T_{end} > 550$ K only an isotropic spectrum (8 lines) with $\tau_{corr} \approx 10^{-10}$ s and an isotropic value of

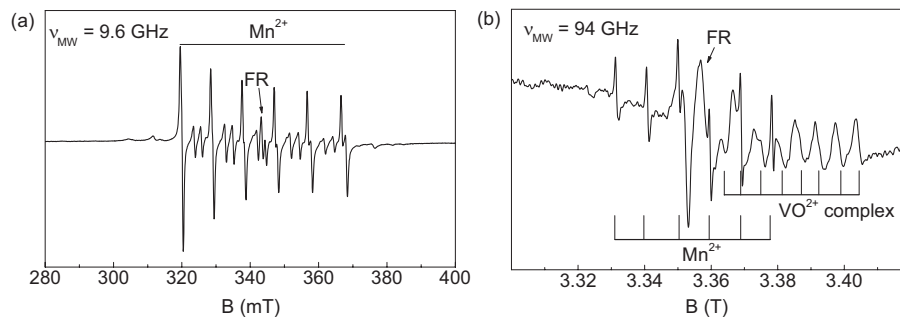


Fig. 2. CW EPR spectra of petroleum rocks from the Boca de Jaruco oilfield at two frequency ranges (a – X-band, b – W-band) due to FR, VP signals and divalent manganese complexes. The type and spectroscopic parameters of these PCs are discussed in details in the text

| | Concentration of FR, spin/g | Concentration of VP complex, spin/g | Parameters of describing of the FR line in the X-band. | Parameters of describing of the FR line in the W-band. |
|---------------|-------------------------------|-------------------------------------|--|---|
| Ashalchinskoe | $(1.1 \pm 0.2) \cdot 10^{17}$ | $(1.2 \pm 0.2) \cdot 10^{18}$ | $g=2.0036$; $G:L = 61:39$; $\Delta H_{pp} = 0.64$ mT | |
| Salym | $(8.0 \pm 0.9) \cdot 10^{18}$ | Not detected | $g=2.0023$; $G:L = 53:47$; $\Delta H_{pp} = 0.31$ mT | $g_{ } = 2.00235$, $g_{\perp} = 2.00145$ $\Delta H_{pp}(L) = 0.38$ mT |
| Cuban | $(4.3 \pm 0.8) \cdot 10^{16}$ | $(1.4 \pm 0.2) \cdot 10^{17}$ | $g=2.0018$; $G:L = 34:66$; $\Delta H_{pp} = 0.55$ mT | |
| Chinese | $(2.8 \pm 0.4) \cdot 10^{17}$ | Not detected | $g=2.0042$; $G:L = 19:81$; $\Delta H_{pp} = 0.51$ mT | $g_{ } = 2.0047$, $g_{\perp} = 2.0041$ $\Delta H_{pp}(L) = 0.75$ mT |

Table 3. Concentrations of FR and VP complexes in the studied petroleum samples and parameters of approximation of EPR spectra for FR in the X-band as convolutions of Gaussian (G) and Lorentz (L) lineshapes and as the center of axial symmetry in the W-band

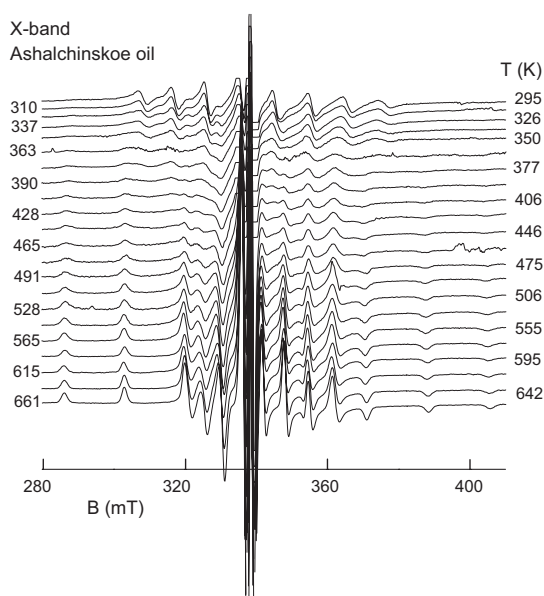


Fig. 3. Changes in the X-band EPR spectrum of the VP complex in the Ashalchinskoe petroleum sample at temperatures $T = 295\text{--}661\text{ K}$

$A \approx 300\text{ MHz}$ is detected in the sample (Gafurov et al., 2018). In this case, the process is temperature-reversible, and the values of the g-factor components do not change within the accuracy of measurements.

Assuming the validity of the Smoluchowski-Stokes-Einstein-Debye equation for PDS (Trukhan et al., 2014):

$$\tau_{\text{bp}} = 4\pi R^3 \eta(T) / 3k_B T, \quad (2)$$

where R is the characteristic size of molecules, $\eta(T)$ is the temperature dependent PDS viscosity, k_B is the Boltzmann constant, and using the experimental values of $\eta(T)$ from (Ilyin et al., 2016), we can estimate the characteristic sizes of molecules containing VP complexes by means of equation (2) as $(0.23 \pm 0.05)\text{ nm}$ at high temperatures ($T < T_{\text{start}}$) and $(1.0 \pm 0.1)\text{ nm}$ at low temperatures ($T > T_{\text{end}}$). That is, the characteristic dimensions of the VP complex during this transition change by a factor of 6–8, which is in good agreement with the accepted scheme of aggregation of asphaltene molecules (Mullins et al., 2014). These results support the model of participation of the VP complexes (at least detected by EPR) in the structures of asphaltene aggregates. We did not perform such temperature measurements in the W-band for lack of a high-temperature resonator.

It should be noted that signals from nickel complexes (nickel porphyrins) cannot be observed in the EPR spectra of PDS, despite their prevalence in PDS (Yakubova et al., 2019). Several assumptions can explain this fact. First, if the nickel is in a tetrahedral configuration, the EPR signal may not be detected. Second, if nickel is located in an octahedral environment that is strongly distorted in the axial direction (in the case of porphyrin complexes), the value of the initial splitting in the zero magnetic field (ZFS, zero-field splitting) can be much higher than the

value for the thermal energy kT , so that only the ground state with $m_s = 0$ is populated (Tayeb Ben et al., 2015).

Figure 4 shows the X-band EPR pulse spectrum for the Ashalchinskoe oil and its simulation using the EasySpin program for Matlab (Stoll, Schweiger, 2006) with the parameters $g_{\perp} = 1.9860$; $g_{\parallel} = 1.9661$; $A_{\perp} = 160\text{ MHz}$; $A_{\parallel} = 470\text{ MHz}$. To detect the ESE spectrum of the VP complex in the initial PDS, it was necessary to lower the temperature down to $T = 250\text{ K}$ while the ESE in asphaltenes and resins isolated from the oil as well as the ESE signal from FR in the initial sample can be detected also at room temperatures.

The values of relaxation times for FR and VP in Ashalchinskoe oil are given in Table 4 demonstrating that the longitudinal relaxation times for VP in the X-band are of 1–2 orders of magnitude shorter than those values for FR. It explains why in a number of samples the ESE signal from VP at room and at elevated temperatures (especially in strong magnetic fields) may not be observed. The data obtained for a large number of samples studied by us contrasts with the results of (Raghunathan, 1991) in which the asphaltenes extracted from the Athabasca (Canada) bitumen were investigated. It was shown (Raghunathan, 1991) that the ESE from VP complexes in the X-band can be detected only at $T < 20\text{ K}$ requiring a usage of expensive cooling system to achieve such low temperatures. We think that this observation is most likely due to the imperfection of the homemade pulsed EPR technique used in (Raghunathan, 1991).

When the temperature decreases (in order to slow down the relaxation processes) it is possible to observe oscillations (Figure 5) on the components of the VP complex spectrum (but not for FR) caused by electron-nuclear interactions. The Fourier-transformed signal of the three-pulse version of ESEEM (Electron Spin

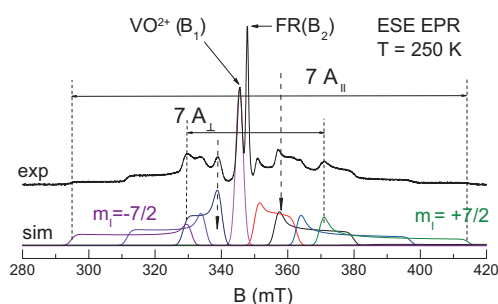


Fig. 4. ESE detected EPR spectrum for the Ashalchinskoe oil at $T = 250\text{ K}$ (exp) and simulation of the VP complex spectrum (sim). Contributions from HFS components with different m_l values are shown

| | VP complex (B_1), μs | FR (B_2), μs |
|----------|-------------------------------------|-----------------------------|
| T_{1e} | 1.7(2) | 23.6(8) |
| T_{2e} | 0.31(4) | 0.30(4) |

Table 4. Values of T_{1e} and T_{2e} from pulse measurements at $T = 250\text{ K}$ in Ashalchinskoe oil at magnetic fields B_1 and B_2 (Figure 4)

Echo Envelope Modulation, (Dikanov, Tsvetkov, 1992; Dzyuba, 2013; Schweiger, Jeschke, 2001) is shown in Figure 6. The ESEEM spectrum clearly shows signals due to the interaction of an electron with protons ($I = 1/2$, a signal at the Larmor frequency of 14.7 MHz) and partially resolved peaks in the frequency range of 0-10 MHz attributed to the interaction with ^{14}N nuclei with $I = 1$ (Deligiannakis et al., 2000) while in the EPR spectra of the samples studied no splittings caused by these nuclei were observed (see also (Gilinskaya, 2008) discussing the rare possibility of observing FR EPR line splittings in the X-band caused by nitrogen nuclei). Thus, ESEEM technique allows one to determine the type of ligand environment (in this case, the presence of ^{14}N nuclei) for vanadyl-porphyrin complexes in the PDS without their extraction.

The relative intensities and exact positions of the peaks in Figure 6 depend on the choice of orientation (B_0 value) and the type(s) of the prevailing VP complexes. The complicated ESEEM spectrum for ^{14}N is due to the existence of not only hyperfine, but also quadrupole interaction characterized by the Q tensor. The paper (Reijerse et al., 1998) is devoted to the interpretation of the results of ESEEM studies of model (synthetic) porphyrins. Determination of components of the Q tensor by electron-nuclear double resonance (ENDOR) directly

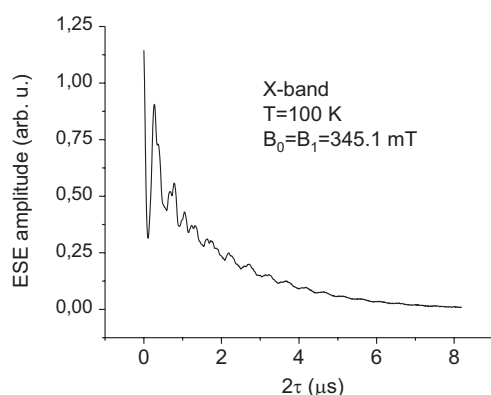


Fig. 5. ESE amplitude decay signal for VP complex in a magnetic field $B_1 = 345.1 \text{ mT}$

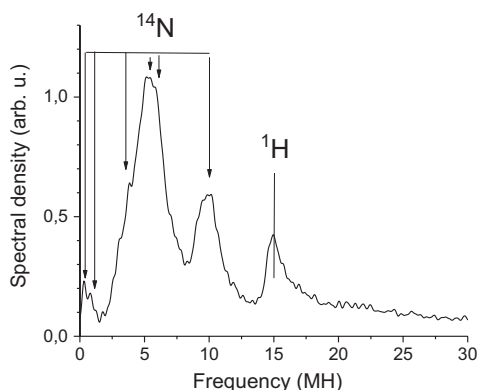


Fig. 6. The Fourier transform of the time dependence of the three-pulse ESEEM for the VP complex in a magnetic field $B_1 = 345 \text{ mT}$

in PDS samples without their processing and extraction is done in (Gracheva et al., 2016). In the present paper double resonance techniques for studying the structure and dynamics of PDS are not considered.

Figure 7 shows a typical ESE spectrum of asphaltenes in the W-band at $T = 100 \text{ K}$ (it is known that T_{1c} in solids decreases with external magnetic field (Abragam, Blieni, 1973)); therefore, the registration of ESE for VP complex in the W-band sometimes requires the use of lower temperatures compared to the X-band). The value of the repetition time of the pulse sequence of $T_{\text{repetition}} = 500 \mu\text{s}$ was chosen in order to increase the intensity of the VP signal comparing to the FR due to the difference in longitudinal relaxation T_1 times (compare with the data in Table 4). The slight difference between the g-factors of FR and VP also allows resolute spectrally these PCs at high frequencies (Figure 7). In addition, due to the higher spectral resolution, the values of the g-tensor components for VP complex can be determined with better accuracy. Figure 8 explains the EPR pattern of the powder spectrum for the VP in the W-band; the arrows show the values of B_0 corresponding to the values of g_{\parallel} and g_{\perp} for the VP complexes.

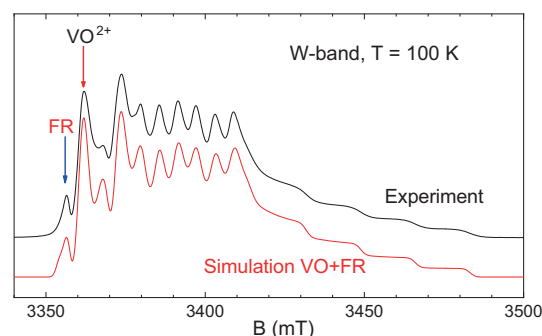


Fig. 7. EPR spectrum of asphaltenes from Ashalchinskoe oil in the pulse mode in the W-band at $T = 100 \text{ K}$ and $T_{\text{repetition}} = 500 \mu\text{s}$. The same graph shows a simulated spectrum obtained by adding the VO^{2+} powder spectrum ($g_{\parallel} = 1.964$, $g_{\perp} = 1.984$, $A_{\parallel} = 16.8 \text{ mT}$, $A_{\perp} = 6.0 \text{ mT}$) and a single free radical line ($g = 2.0036$). The FR and VO^{2+} markers indicate the B_0 values at which the electronic relaxation times were measured for FR and VP

3.3. EPR of FR

It is known that in the X-band the FR EPR spectrum in PDS in most cases is a single line with a width of $\Delta H_{\text{pp}} = (0.4 - 0.7) \text{ mT}$ and an isotropic g-factor in the range of 2.003 ± 0.001 (Yen, Chilingarian, 1994, 2000; Gizatullin et al., 2018) which is conventionally fitted by a standard combination of Gaussian (G) and Lorentzian (L) lineshapes with the same g-factors and approximately the same width (Mukhamatdinov et al., 2018). For example, Figure 9 shows the approximation of the FR EPR line in the Origin program by the Voigt function (convolution of the Lorentz and Gaussian

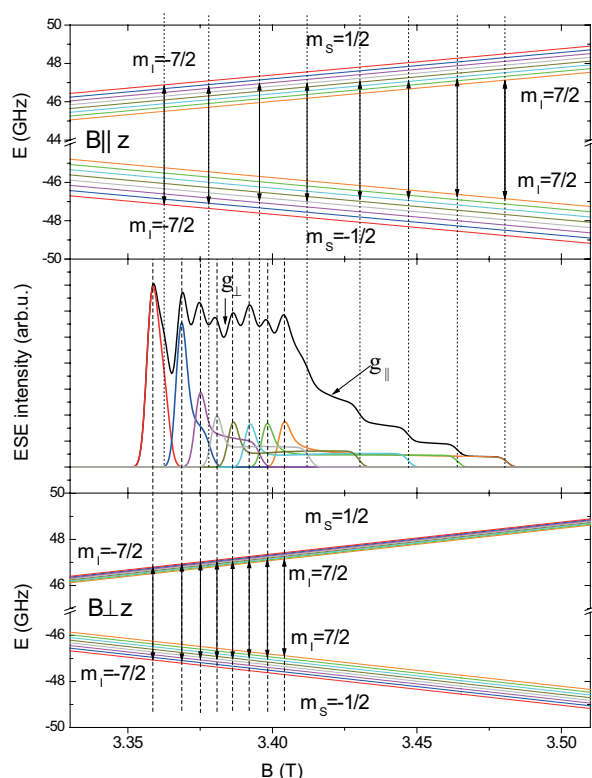


Fig. 8. Energy levels and the corresponding EPR absorption spectrum for the VP complex, calculated for the microwave frequency $\nu = 94$ GHz, $g_{\parallel} = 1.963$, $g_{\perp} = 1.985$, $A_{\parallel} = 470$ MHz, $A_{\perp} = 150$ MHz. Individual contributions from each EPR transition are highlighted in different colors

lineshapes) for the Salym oil. Numerical parameters of approximations for FR are given in Table 3.

Our experience in studies of various PDS in the W-band (Volodin et al., 2013) shows that the FR spectra in the vast majority of cases have an asymmetric lineshape (the left, low-field wing is “prolonged”). Thus, the typically accepted description of EPR spectra for FR in the X-band does not allow describing the EPR spectrum at higher frequencies.

The authors of (Di Mauro et al., 2005) drew attention to the asymmetry of the EPR line of “free” radicals in asphaltenes from Arabian and Colombian deposits in the W-band. They failed to describe the experimental data with an anisotropic g-factor for single PC and, as a result, it was assumed that the EPR spectrum is due to

the presence of two (or more) different PC EPR lines of which are partially resolved in strong magnetic fields. While agreeing with this interpretation, it should be noted that for some PDS samples it is possible to describe the FR signal by a single PC.

For example, EPR spectra for Salym and Chinese oils can be fitted in both frequency ranges using a single set of parameters for the center of axial symmetry (Table 3, Figure 10). Additional arguments in favor of describing the EPR signal by a single PC are (1) the independence of the relaxation characteristics (T_{1FR} and T_{2FR} curves) from the choice of the exact value of the magnetic field along the EPR spectrum and (2) the independence of the EPR spectrum from temperature changes (in the range of 20–300 K). It is noteworthy that for all petroleum samples studied in this work (not to mention asphaltenes), the ESE signal in the W-band can be observed at room temperatures.

We have not been able to describe satisfactorily the FR spectra for Ashalchinskoe and Cuban oil using the PC of axial and even rhombic symmetry. It should be mentioned that these samples, in contrast to Salym and Chinese oils, contain other types of PCs (Figure 2, Table 3). It is also known that an increase in the concentration of heteroatoms (primarily oxygen and sulfur) leads to a shift of EPR lines to low magnetic fields (Gizatullin et al., 2018; Khasanova et al., 2017; and the literature cited there). Detailed studies of the effect of heteroatoms and other PCs on the FR spectral characteristics were not performed in this paper.

3.4. Measurement of electronic relaxation times of VP complex and FR in asphaltene fractions in the W-band

As noted above, the position, shape and intensity of CW EPR lines for FR and VP in the X-band are a kind of fingerprints for classifying hydrocarbon raw materials from various oilfields and allow controlling the processes of PDS treatment (Yen, Chilingarian, 1994, 2000; Mehrabi-Kalajahi et al., 2018). It is logical to assume that the electronic relaxation characteristics are also parameters that are sensitive to changes in the chemical and coordination environment of the PC in PDS.

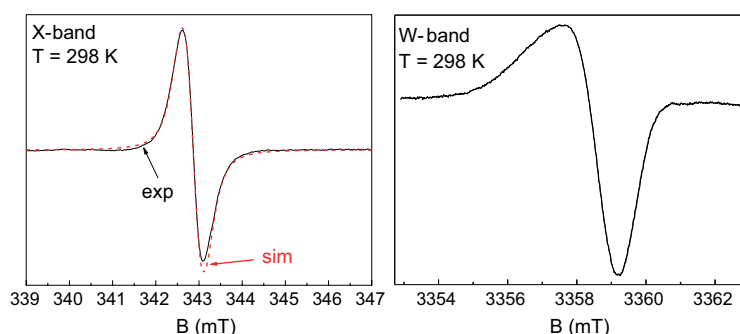


Fig. 9. EPR spectrum (exp) of the Salym oil in the X-band (left) and W-band (right) with its approximation by the Voigt line (sim) with the parameters described in the text (Table 3)

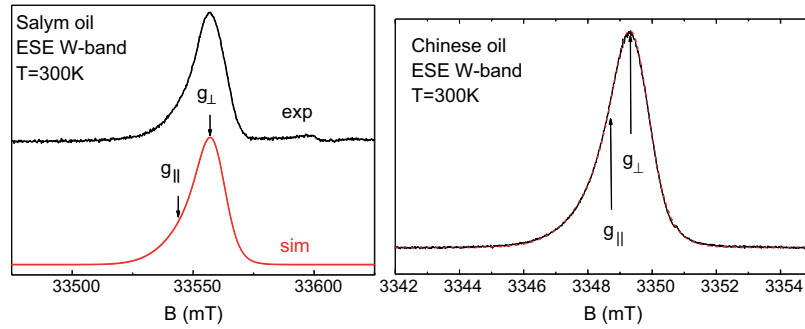


Fig. 10. Echo-detected EPR spectra of samples of Salym (left) and Chinese (right) petroleum in the W-band at room temperature and their description by the center of axial symmetry with g_{\parallel} and g_{\perp} (Table 3). Experimental data are denoted as exp (black lines), approximation curves as sim (red lines)

The objects of the study were 12 different asphaltene powders (section 2.1) extracted from technical bitumen and heavy oils. The measurements were performed in the W-band at $T = 300$ K. As in the case of X-band studies, it was found that for FR the longitudinal relaxation times of T_{1FR} are in the range of 20–100 ms, significantly varying from sample to sample, while for VP complex, the values of T_{1VP} are significantly shorter (in the range of 1.0–1.8 ms, Figure 11).

The times of VP transverse relaxation in asphaltenes are also significantly shorter than for FR. In all samples, without taking into account the modulation effects, a monoexponential decay of the transverse magnetization was observed with characteristic T_{2VP} times in the range of 80–220 ns.

The character of the T_{2FR} transverse magnetization decay differs from the monoexponential one (Figure 12) and can be well described by the expression (Mamin et al., 2016):

$$I_{echo} = M_{FR} \cdot \exp\left(-\frac{2\tau}{T_{2FR}}\right) \cdot \exp(-m \cdot \tau^2), \quad (3)$$

where M_{FR} is a coefficient proportional to the FR concentration, and m is a parameter that takes into account the spectral diffusion in the FR. Table 5 shows data on measuring the relative concentration of PCs in the X-band.

All the obtained relaxation data are well grouped around the following straight lines (Figure 13):

$$m T_{1CP} \propto (3.0 \pm 0.4) \cdot T_{2VO}^{-1}, \quad (4)$$

$$T_{2CP}^{-1} \propto (0.43 \pm 0.08) \cdot T_{2VO}^{-1}. \quad (5)$$

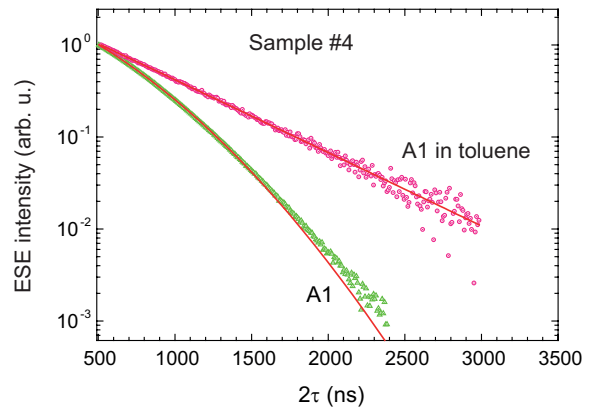


Fig. 12. ESE amplitude decay signal for FR in the W-band for sample No. 4 at room temperature. The dots represent experimental data, solid lines show the results of approximation by (2) with $m = 0$ in toluene solution (upper line, dissolution in the ratio A1:toluene = 1:10 by volume) and $m = 3.6 \cdot 10^{-6} \text{ ns}^{-2}$ for the undissolved fraction (lower line)

| Sample | A _{init} | A1 | A2 |
|--------|-------------------|-----------|-------------|
| N1 | 1.9 ± 0.1 | 3.6 ± 0.2 | 1.4 ± 0.1 |
| N2 | 49 ± 2 | 60 ± 3 | 28 ± 2 |
| N3 | 0.73 ± 0.05 | 0.7 ± 0.1 | 0.7 ± 0.1 |
| N4 | 1.15 ± 0.09 | 1.0 ± 0.1 | 0.50 ± 0.05 |

Table 5. Relative concentrations of “free” radicals and vanadyl-porphyrin complexes (C_{FR}/C_{VP}) in the studied samples of asphaltenes (from measurements in the X-band at $T = 300$ K)

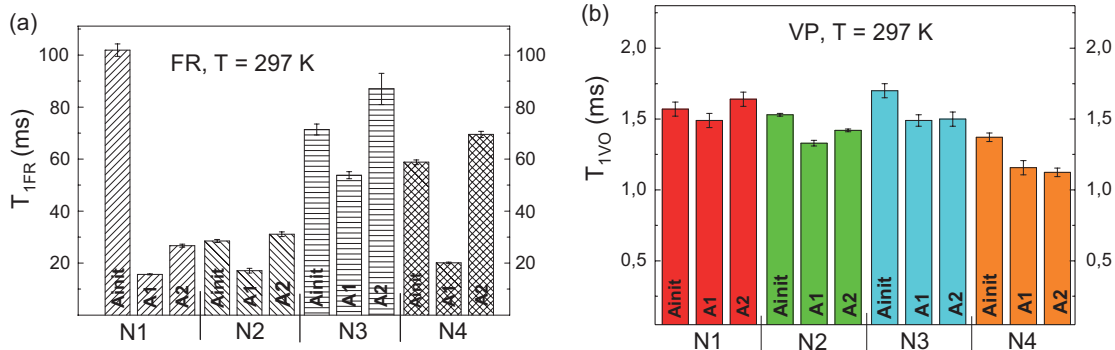


Fig. 11. Longitudinal relaxation times T_1 for FR (a) and VP (b) at $T = 297$ K in the W-band for 12 studied asphaltene samples

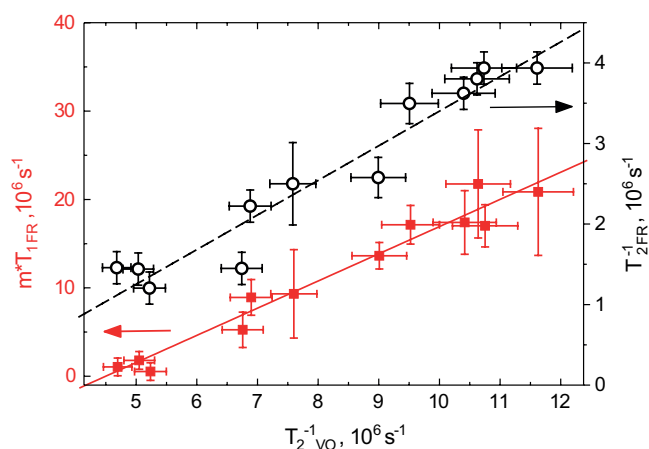


Fig. 13. Dependence of the product of the longitudinal relaxation time for FR by the spectral diffusion coefficient on the transverse relaxation rate for VP (red squares, left ordinate axis) and the dependence of the transverse relaxation rate FR on the transverse relaxation rate of vanadyl porphyrins (open circles, right ordinate axis) for 12 samples studied

From the analysis of relaxation times it was found (Mamin et al., 2016) that the acceleration of the transverse relaxation process according to (3) is caused by the presence of vanadyl-porphyrin molecules in the close vicinity (1–3 nm) of the FR. This discovery, in our opinion, shows a step towards understanding the structure of asphaltenes and to the role that vanadium complexes play in their aggregation. Note that when samples of asphaltenes are dissolved in organic solvents (for example, in toluene in the ratio of asphaltene: toluene $\geq 1:10$ by volume and higher) the magnetization decay curves convert to a typical monoexponential form (Figure 12). The presented data once again support the need to study PDS under conditions close to native (*in situ*), and not in solutions or using model samples – the obtained dynamic characteristics on model samples and solutions may differ significantly from those for real petroleum systems. Here it is appropriate to emphasize again the features (advantages) of EPR techniques that allow to study both native PDS and their components and solutions.

Such “accelerations” of T_{2FR} curves were not described for PDS before our experiments (Mamin et al., 2016). The fact that we were not able to observe them in the X-band seems to be related to the overlap of the FR and VP complex spectra at lower frequencies (Figures 2, 4, 7).

Conclusion

In this paper, we have tried to demonstrate some of the capabilities of pulsed and high-frequency EPR for studying petroleum disperse systems. Among the results of the work the following items can be emphasized.

1. It is found that in asphaltenes, as well as in a large number of samples of light and heavy oils it is possible to observe electron spin echo signal of native paramagnetic centers at room temperatures and in a strong magnetic fields ($B = 3.4$ T). This makes it possible to apply a wide

toolkit of pulsed EPR techniques to study unfractionated petroleum disperse systems, high-molecular components of petroleum disperse system and their solutions, identify the types and values of electron-nuclear interactions, track changes in time parameters that characterize complex hydrocarbon systems under external influence, etc., even without the use of cryogenic technology.

2. Analysis of the transverse magnetization decay curve (ESEEM) on the components of paramagnetic vanadyl-porphyrin petroleum disperse system complexes makes it possible to identify electron-nuclear interactions with the ^{14}N and ^1H environment nuclei under *in situ* conditions, while these hyperfine interactions cannot be detected in the EPR spectra of native petroleum disperse system samples due to inhomogeneous line broadening.

3. The use of high-frequency EPR makes it possible (at least partially) to spectrally separate contributions from various paramagnetic centers, and to determine their spectral and relaxation characteristics more precisely.

4. It was found that the shape of the EPR signal of “free” organic radicals in the studied oil and asphaltene samples in the W-band cannot be described by an isotropic single line, as in the X-band. Thus, the results and conclusions of a number of studies on the analysis of changes in the shape of the EPR line in petroleum disperse system in the X-band under external influence should be reinterpreted.

5. At the same time, in contrast to the results of (Di Mauro et al., 2005), it is shown that in a number of petroleum disperse system, EPR lines of “free” organic radicals can be attributed to single paramagnetic center of axial symmetry.

6. Due to spectral resolution of lines of various paramagnetic centers in the petroleum disperse system in strong magnetic fields ($B = 3.4$ T, W-band), the effect of increasing the rates of electronic transverse relaxation of paramagnetic centers native for the petroleum disperse

system asphaltenes is found. The obtained data are interpreted in the framework of a model of spectral diffusion between fast- and slow-relaxing paramagnetic centers in supramolecular complexes of asphaltenes.

The authors hope that further research will allow to reveal new possibilities of EPR to follow dynamic and structural properties of petroleum disperse system like in biomolecular systems (Qin, Warncke, 2015a, b).

Acknowledgments

The authors are thankful to D.T. Sitdikov, M.A. Volodin, A.V. Vakhin, Yu.M. Ganeeva and T.N. Yusupova for their help in carrying out measurements and preparing samples, T.B. Biktagirov for a number of theoretical calculations, V.I. Morozov for discussing the results obtained, A.V. Dooglav for careful reading of the manuscript, valuable comments and for help with the text translation.

The authors thank the reviewers for the opportunity to correct and improve the manuscript.

The work was supported by the RSF grant 19-12-00332.

References

- Abragam A., Bleaney B. (1970). *Electron Paramagnetic Resonance of Transition Ions*. Oxford: Clarendon press.
- Abyzgildin Yu.N., Mikhailyuk Yu.N., Yarullin K.S., Rostovskaya A.A. (1977). Porphyrins and metal porphyrin complexes of oils. Moscow: Nauka, 88 p. (In Russ.)
- Acevedo S., Guzman K., Ocanto O. (2010). Determination of the number average molecular mass of asphaltenes (Mn) using their soluble A2 fraction and the vapor pressure osmometry (VPO) technique. *Energy & Fuels*, 24(3), pp. 1809–1812. <https://doi.org/10.1021/ef9012714>
- Al-Muntaser A.A., Varfolomeev M.A., Suwaid M.A. et al. (2020). Hydrothermal upgrading of heavy oil in the presence of water at sub-critical, near-critical and supercritical conditions. *Journal of Petroleum Science and Engineering*, 184, 106592. <https://doi.org/10.1016/j.petrol.2019.106592>
- Alexandrov A.S., Ivanov A.A., Archipov R.V., Gafurov M.R., Tagirov M.S. (2019). Pulsed NMR spectrometer with dynamic nuclear polarization for weak magnetic fields. *Magnetic Resonance in Solids*, 21(2), pp. 19203 (1–6). <https://doi.org/10.26907/mrsej-19203>
- Cui Q., Ma X., Nakano K., Nakabayashi K., Miyawaki J., Al-Mutairi A. et al. (2018). Hydrotreating reactivities of atmospheric residues and correlation with their composition and properties. *Energy & Fuels*, 32(6), pp. 6726–6736. <https://doi.org/10.1021/acs.energyfuels.8b01150>
- Cui Q., Nakabayashi K., Ma X., Ideta K., Miyawaki J., Marafi A.M. et al. (2017). Examining the molecular entanglement between V=O complexes and their matrices in atmospheric residues by ESR. *RSC advances*, 7(60), pp. 37908–37914. <https://doi.org/10.1039/C7RA06436E>
- Davydov V.V., Dudkin V.I., Myazin N.S., Rud' V.Yu. (2018). Peculiarity of the Nuclear Magnetic Resonance Method Application for the Liquid Medium Flow Parameters Control. *Applied Magnetic Resonance*, 49(7), pp. 665–679. <https://doi.org/10.1007/s00723-018-0994-1>
- Deligiannakis Y., Louloudi M., & Hadjiliadis N. (2000). Electron spin echo envelope modulation (ESEEM) spectroscopy as a tool to investigate the coordination environment of metal centers. *Coordination Chemistry Reviews*, 204(1), pp. 1–112. [https://doi.org/10.1016/S0010-8545\(99\)00218-0](https://doi.org/10.1016/S0010-8545(99)00218-0)
- Di Mauro E., Guedes, C.L.B., Nascimento O.R. (2005). Multifrequency (X-band to W-band) CW EPR of the organic free radical in petroleum asphaltene. *Applied Magnetic Resonance*, 29(4), pp. 569–575. <https://doi.org/10.1007/BF03166333>
- Dickson F.E., Kunesch, C.J., McGinnis E.L., Petrakis L. (1972). Use of electron spin resonance to characterize the vanadium (IV)-sulfur species in petroleum. *Anal. Chem.*, 44(6), pp. 978–981. <https://doi.org/10.1021/ac60314a009>
- Dikanov S.A., Tsvetkov Y.D. (1992). *Electron Spin-Echo Envelope Modulation (ESEEM) Spectroscopy*. USA: CRC Press, 432 p.
- Dolomatov M., Gafurov M., Rodionov A., Mamin G., González L.M., Vakhin A., Petrov A., Bakhtizin R., Khairudinov I., Orlinskii, S. (2018). Low-temperature thermal decomposition of heavy petroleum distillates: interconnection between the electrical properties and concentration of paramagnetic centres. *IOP Conf. Ser.: Earth Environ. Sci.*, 155, 012007. <https://doi.org/10.1088/1755-1315/155/1/012007>
- Dolomatov M.U., Rodionov A.A., Gafurov M.R., Petrov A.V., Biktagirov T.B., Bakhtizin R.Z., Makarchikov S.O., Khairudinov I.Z. and Orlinskii S.B. (2016). Concentration of paramagnetic centres at low-temperature thermal destruction of asphaltenes of heavy petroleum distillates. *Magnetic Resonance in Solids*, 18, 16101. <http://mrsej.kpfu.ru/contents.html#16101>
- Dzuba S.A. (2013). Structural studies of biological membranes using ESEEM spectroscopy of spin labels and deuterium substitution. *J Struct Chem*, 54, pp. 1–15. <https://doi.org/10.1134/S0022476613070019>
- Eaton, G.R., Eaton, S.S., Barr, D.P., Weber, R.T. (2010). *Quantitative EPR*. Vienna: Springer-Verlag Wien. <https://doi.org/10.1007/978-3-211-92948-3>
- Gafurov M.R., Volodin M.A., Rodionov et al. (2018). EPR study of spectra transformations of the intrinsic vanadyl-porphyrin complexes in heavy crude oils with temperature to probe the asphaltenes' aggregation. *Journal of Petroleum Science and Engineering*, 166, pp. 363–368. <https://doi.org/10.1016/j.petrol.2018.02.045>
- Galukhin A., Bolmatenkov D., Osin Y. (2018). Heavy oil oxidation in the nano-porous medium of synthetic opal. *RSC Adv.*, 8, pp. 18110–18116. <https://doi.org/10.1039/C8RA02822B>
- Garif'yanov N.S., Kozyrev B.M. (1956). Paramagnetic resonance in anthracite and other carbon-containing substances. *Zh. Eksp. Teor. Fiz.*, 30(2), pp. 272–276. (In Russ.)
- Gilinskaya L.G. (2008). EPR spectra of V(IV) complexes and the structure of oil porphyrins. *J Struct Chem*, 49, pp. 245–254. <https://doi.org/10.1007/s10947-008-0120-6>
- Gizatullin B., Gafurov M., Vakhin et al. (2019). Native Vanadyl Complexes in Crude Oil as Polarizing Agents for In Situ Proton Dynamic Nuclear Polarization. *Energy & Fuels*, 33(11), pp. 10923–10932. <https://doi.org/10.1021/acs.energyfuels.9b03049>
- Gizatullin B., Gafurov, M., Rodionov A., Mamin, G., Mattea, C., Stapf, S., Orlinskii, S. (2018). Proton–Radical Interaction in Crude Oil – A Combined NMR and EPR Study. *Energy & Fuels*, 32(11), pp. 11261–11268. <https://doi.org/10.1021/acs.energyfuels.8b02507>
- Gracheva I., Gafurov M., Mamin G., Biktagirov T., Rodionov A., Galukhin V., Orlinskii S.B. (2016). ENDOR Study of Nitrogen Hyperfine and Quadrupole Tensors in Vanadyl Porphyrins of Heavy Crude Oils. *Magnetic Resonance in Solids*, 18, 16102. <http://mrsej.kpfu.ru/contents.html#16102>
- Gutowsky H., Roger Ray B., Rutledge R., Unterberger R. (1958). Carbonaceous Free Radicals in Crude Petroleum. *J. Chem. Phys.*, 28, pp. 744–745. <https://doi.org/10.1063/1.1744250>
- Ilyasov A.V. (1962). Determination of vanadium content in oils and petroleum products by EPR method. *Chemistry and Technology of Fuels and Oils*, 9, pp. 63–67. (In Russ.)
- Ilyasov A.V., Garif'yanov N.S., Ryzhmanov Yu.S. (1961). Electron paramagnetic resonance in some types of natural oils and their heavy fractions. *Chemistry and Technology of Fuels and Oils*, 1, pp. 28–31. (In Russ.)
- Ilyin S.O., Arinina M.P., Polyakova M.Y. et al. (2016). Rheological comparison of light and heavy crude oils. *Fuel*, 186, pp. 157–167. <https://doi.org/10.1016/j.fuel.2016.08.072>
- Khasanova N.M., Gabdrakhmanov D.T., Kayukova G.P., Morozov V.P., Mikhaylova A.N. (2017). EPR study of hydrocarbon generation potential of organic-rich domanik rocks. *Magnetic Resonance in Solids*, 19(1), 17102. <http://mrsej.ksu.ru/contents.html#17102>
- Mamin G., Gafurov M., Yusupov R., Gracheva I., Ganeeva Y., Yusupova T., Orlinskii S.B. (2016). Toward the Asphaltene Structure by Electron Paramagnetic Resonance Relaxation Studies at High Fields (3.4 T). *Energy & Fuels*, 30(9), pp. 6942–6946. <https://doi.org/10.1021/acs.energyfuels.6b00983>
- Martyanov O.N., Larichev Y.V., Morozov E.V., Trukhan S.N., Kazarian S.G. (2017). The stability and evolution of oil systems studied via advanced methods in situ. *Russ. Chem. Rev.*, 86, pp. 999–1023. <https://doi.org/10.1070/RCR4742>
- Mehrabi-Kalajahi S.S., Varfolomeev M.A., Yuan C. et al. (2018). EPR as a complementary tool for the analysis of low-temperature oxidation reactions of crude oils. *Journal of Petroleum Science and Engineering*, 169, pp. 673–682. <https://doi.org/10.1016/j.petrol.2018.05.049>
- Mukhamatdinov I., Gafurov M., Kemalov A., et al. (2018). Study of the oxidized and non-oxidized bitumen modified with additive «Adgezolin» by using electron paramagnetic resonance. *IOP Conf. Ser.: Earth Environ. Sci.*, 155, 012004. <https://doi.org/10.1088/1755-1315/155/1/012004>
- Mukhamatdinov I.I., Salih I.Sh.S., Rakhmatullin I.Z., Sitnov S.A., Laikov A.V., Klochkov V.V., Vakhin A.V. (2020). Influence of Co-based catalyst on

- subfractional composition of heavy oil asphaltenes during aquathermolysis, *Journal of Petroleum Science and Engineering*, 186, 106721. <https://doi.org/10.1016/j.petrol.2019.106721>
- Mullins O., Pomerantz A.E., Zuo J., Dong C., Annu J. (2014). Downhole fluid analysis and asphaltene science for petroleum reservoir evaluation. *Rev. Chem. Biomol. Eng.*, 5, pp. 325–345. <https://doi.org/10.1146/annurev-chembioeng-060713-035923>
- Murav'ev F.A., Vinokurov V.M., Galeev A.A., Bulka G.R., Nizamutdinov N.M., Khasanova N.M. (2006). Paramagnetism and nature of dispersed organic matter in the Permian deposits of Tatarstan. *Georesursy = Georesources*, 2(19), pp. 40–45. (In Russ.)
- Nesterov I.I., Alexandrov V.M., Ponomarev A.A., Zavatsky M.D., Lobodenko E.I., Kobylinskiy D.A., Kadyrov M.A. (2019). Experimental studies of radical reactions of hydrocarbons conversion. *Oil and Gas Studies*, 4, pp. 57–69. (In Russ.) <https://doi.org/10.31660/0445-0108-2019-4-57-69>
- O'Reilly, D. (1958). Paramagnetic Resonance of Vanadyl Etioporphyrin I. *J. Chem. Phys.*, 29(5), pp. 1188–1189. <https://doi.org/10.1063/1.1744684>
- Piccinato M., Guedes C., Di Mauro E. (2012). Petroleum Asphaltenes. *Crude Oil Emulsions – Composition Stability and Characterization*. Ed. M. Abdul-Raouf. Rjeka: InTech, pp. 147–168.
- Ponomarev A.A. (2019). The mechanism of cracking hydrocarbons in electromagnetic fields – to the question of oil in Bazhenov formation. *Oil and Gas Studies*, 1, pp. 14–18. (In Russ.) <https://doi.org/10.31660/0445-0108-2019-1-14-18>
- Qin P., Warncke K. (2015a). Electron Paramagnetic Resonance Investigations of Biological Systems by Using Spin Labels, Spin Probes, and Intrinsic Metal Ions. Part A. *Methods in Enzymology*, 563, pp. 2–684.
- Qin P., Warncke K. (2015b). Electron Paramagnetic Resonance Investigations of Biological Systems by Using Spin Labels, Spin Probes, and Intrinsic Metal Ions. Part B. *Methods in Enzymology*, 564, pp. 2–613.
- Raghunathan P. (1991). Evidence for fractal dimension in asphaltene polymers from electron-spin-relaxation measurements. *Chem. Phys. Lett.* 182, pp. 331–335. [https://doi.org/10.1016/0009-2614\(91\)80224-L](https://doi.org/10.1016/0009-2614(91)80224-L)
- Ramachandran V., van Tol, J., McKenna A., Rodgers R., Marshall A., Dalal N. (2015). High Field Electron Paramagnetic Resonance Characterization of Electronic and Structural Environments for Paramagnetic Metal Ions and Organic Free Radicals in Deepwater Horizon Oil Spill Tar Balls. *Anal. Chem.*, 87(4), pp. 2306–2313. <https://doi.org/10.1021/ac504080g>
- Reijerse E.J., Tyryshkin A.M., Dikanov S.A. (1998). Complete determination of nitrogen quadrupole and hyperfine tensors in an oxovanadium complex by simultaneous fitting of multifrequency ESEEM powder spectra. *Journal of Magnetic Resonance*, 131(2), pp. 295–309. <https://doi.org/10.1006/jmre.1997.1339>
- Safieva R.Z. (2004). Chemistry of oil and gas. Petroleum Dispersed Systems: Composition and Properties. Part 1. Moscow: Gubkin Russian State University of Oil and Gas, 112 p. (In Russ.)
- Sapunov V.A., Denisov A.Y., Saveliev D.V. et al. (2016). New vector/scalar Overhauser DNP magnetometers POS-4 for magnetic observatories and directional oil drilling support. *Magnetic Resonance in Solids*, 18(2), 16209. <http://mrsej.kpfu.ru/contents.html#16209>
- Sapunov V.A., Kashin I.V., Ushakov V.A. et al. (2019). Little-known aspects of Overhauser DNP at zero and low magnetic fields stimulated by parallel electron pumping of nitroxide radicals solutions. *AIP Conf. Proc.*, 2174, 020112. <https://doi.org/10.1063/1.5134263>
- Schweiger A., Jeschke G. (2001). Principles of Pulse Electron Paramagnetic Resonance. Oxford: OUP.
- Stoll S., Schweiger A. (2006). EasySpin, a comprehensive software package for spectral simulation and analysis in EPR. *Journal of Magnetic Resonance*, 178, pp. 42–55. <https://doi.org/10.1016/j.jmr.2005.08.013>
- Syunyaev Z.I. (1980). Concentration of complex structural units in disperse petroleum systems, and methods for regulation of this concentration. *Chem Technol Fuels Oils*, 16, pp. 484–489. <https://doi.org/10.1007/BF00726762>
- Syunyaev Z.I., Safieva R.Z., Syunyaev R.Z. (1990). Petroleum dispersed systems. Moscow: Chemistry, 224 p. (In Russ.)
- Tayeb Ben K., Delpoux O., Barbier J., Marques J., Verstraete J., Vezin H. (2015). Applications of Pulsed Electron Paramagnetic Resonance Spectroscopy to the Identification of Vanadyl Complexes in Asphaltene Molecules. Part 1: Influence of the Origin of the Feed. *Energy & Fuels*, 29(7), pp. 4608–4615. <https://doi.org/10.1021/acs.energyfuels.5b00733>
- Trukhan S., Yudanov V., Gabrienko A., Subramani V., Kazarian S., Martyanov O. (2014). In Situ Electron Spin Resonance Study of Molecular Dynamics of Asphaltenes at Elevated Temperature and Pressure. *Energy & Fuels*, 28(10), pp. 6315–6321. <https://doi.org/10.1021/ef5015549>
- Vakhin A.V., Aliev F.A., Mukhamatdinov I.I., Sitnov S.A., Sharifullin A.V., Kudryashov S.I., Afanasiev I.S., Petrashov O.V., Nurgaliev D.K. (2020). Catalytic Aquathermolysis of Boca de Jaruco Heavy Oil with Nickel-Based Oil-Soluble Catalyst. *Processes*, 8(5), 532. <https://doi.org/10.3390/pr8050532>
- Volodin M.A., Mamin G.V., Izotov V.V., & Orlinskii S.B. (2013). High-frequency EPR study of crude oils. *J. Phys.: Conf. Ser.*, 478, 012003. <https://doi.org/10.1088/1742-6596/478/1/012003>
- Wang W., Ma Y., Li S., Shi J., Teng J. (2016). Effect of Temperature on the EPR Properties of Oil Shale Pyrolysates. *Energy & Fuels*, 30(2), pp. 830–834. <https://doi.org/10.1021/acs.energyfuels.5b02211>
- Yakubov M.R., Milordov D.V., Yakubova S.G., Morozov V.I. (2017). Vanadium and paramagnetic vanadyl complexes content in asphaltenes of heavy oils of various productive sediments. *Petroleum Science and Technology*, 35(14), pp. 1468–1472. <https://doi.org/10.1080/10916466.2017.1344708>
- Yakubova S.G., Abilova G.R., Tazeeva, E.G., Borisova Y.Y., Milordov D.V., Mironov N.A., Yakubov M.R. (2019). Distribution of Vanadium and Nickel in the Case of Two-Step Solvent Fractionation of Asphaltenes of Heavy Oils. *Petroleum Chemistry*, 59(1), pp. S30–S36. <https://doi.org/10.1134/S0965544119130140>
- Yen T., Chilingarian G. (1994). Asphaltenes and asphalts. 1. Developments in petroleum science. 40A. New York: Elsevier. [https://doi.org/10.1016/S0376-7361\(09\)70248-1](https://doi.org/10.1016/S0376-7361(09)70248-1)
- Yen T., Chilingarian G. (2000). Asphaltenes and asphalts, 2. Developments in petroleum science. 40 B. New York: Elsevier.
- Yen T.F., Erdman J.G., Saraceno A.J. (1962). Investigation of the Nature of Free Radicals in Petroleum Asphaltenes and Related Substances by Electron Spin Resonance. *Analytical Chemistry*, 34(6), pp. 694–700. <https://doi.org/10.1021/ac60186a034>
- Zavoisky E. (1945). Paramagnetic Relaxation of Liquid Solutions for Perpendicular Fields. *Journal of Physics* (Academy of Sciences of the USSR), 9(3), pp. 211–216.
- Zhang Y., Siskin M., Gray M.R., Walters C.C., Rodgers R.P. (2020). Mechanisms of Asphaltene Aggregation: Puzzles and a New Hypothesis. *Energy & Fuels*, 34(8), pp. 9094–9107. <https://doi.org/10.1021/acs.energyfuels.0c01564>
- Zhao X., Xu, C., Shi Q. (2015). Porphyrins in Heavy Petroleum: A Review. In: Xu C., Shi Q. (ed.) Structure and Modeling of Complex Petroleum Mixtures. Structure and Bonding, 168. Springer, Cham. https://doi.org/10.1007/430_2015_189

About the Authors

Marat R. Gafurov – Dr. Sci. (Physics and Mathematics), Leading Researcher, Deputy Director for Research, Institute of Physics, Kazan Federal University
16a Kremlevskaya st., Kazan, 420008, Russian Federation

Andrey A. Ponomarev – Post-graduate student, Tyumen Industrial University
38 Volodarsky st., Tyumen, 625000, Russian Federation

Georgiy V. Mamin – Cand. Sci. (Physics and Mathematics), Associate Professor, Department of Quantum Electronics and Radiospectroscopy, Institute of Physics, Kazan Federal University
18 Kremlevskaya st., Kazan, 420008, Russian Federation

Alexander A. Rodionov – Electronic engineer, Department of Quantum Electronics and Radiospectroscopy, Institute of Physics, Kazan Federal University
18 Kremlevskaya st., Kazan, 420008, Russian Federation

Fadis F. Murzakhanov – Post-graduate student, Institute of Physics, Kazan Federal University
18 Kremlevskaya st., Kazan, 420008, Russian Federation

Tajik Arash – Postgraduate Student, Institute of Geology and Petroleum Technologies, Kazan Federal University
4 Kremlevskaya st., Kazan, 420008, Russian Federation

Sergey B. Orlinskii – Cand. Sci. (Physics and Mathematics), Associate Professor, Department of Quantum Electronics and Radiospectroscopy, Institute of Physics, Kazan Federal University
18 Kremlevskaya st., Kazan, 420008, Russian Federation

*Manuscript received 9 June 2020;
Accepted 3 November 2020; Published 11 December 2020*

